# Preparation, Characterization and Performance Study of Poly(isobutylene-alt-maleic anhydride) [PIAM] and Polysulfone [PSf] Composite Membranes before and after Alkali Treatment

Mahesh Padaki,[†] Arun M. Isloor,*,[†] Ganesh Belavadi,[†] and K. Narayan Prabhu[‡]

[†]Membrane Technology Division, Department of Chemistry, and [‡]Department of Metallurgical and Materials Engineering, National Institute of Technology—Karnataka, Surathkal, Mangalore 575 025, India

**ABSTRACT:** Recently, nanofiltration (NF) membranes have been drawing much attention in the field of filtration and the purification process of water/industrial effluents, because of their energy efficiency and low cost. Although reverse osmosis (RO) membranes are widely used in present desalination units, NF membranes are considered as "future membranes" for desalination, because of the low operating pressure. In the present paper, we hereby report the synthesis of a new composite NF membranes of poly(isobutylene-alt-maleic anhydride) (PIAM) with polysulfone, using a diffusion-induced phase separation (DIPS) method. The anhydride groups were converted to acid group by alkaline treatment. Newly prepared composite membranes were characterized by Fourier transform infrared spectroscopy (FT-IR), scanning electron microscopy (SEM), and differential scanning calorimetry (DSC) studies. The membranes were tested for salt rejection and water swelling. The resulted NF membranes exhibited significantly enhanced water permeability while retaining high salt rejection. The flux and rejection rate of the NF membrane to $Na_2SO_4$ (500 ppm) reached to 11.73 L/(m$^2$ h) and 49% rejection under 1 MPa and also 70:30 composition of the membrane showed 54% water swelling; contact angle measurement, ion exchange capacity, and water uptake of the membrane were recorded.

## ■ INTRODUCTION

Pressure-driven separations are wonderful separation techniques, in particular, membrane technology is widely applicable in many areas, such as chemical and biochemical processes, stream separation, seawater desalination, removal of heavy metals from waste effluents, and purification of potable water.[1−5] In particular, nanofiltration (NF) and reverse osmosis (RO) are more powerful tools widely used in desalination and purification processes. The porous membrane is a major tool in both NF and RO techniques. A membrane is an interphase between two adjacent phases acting as a selective barrier, regulating the transport of substances between the two compartments. It is believed that, in RO and NF membranes, water molecules (0.27 nm) permeate, while hydrated salt ions (e.g., $Na^{1+}$ 0.72 nm in diameter) are rejected.[6] The transfer mechanism of NF involves both pore flow and solution diffusion as in RO. NF membranes especially offer high rejection of organic molecules with molecular weights ranging from 100 Da to 1000 Da and multivalent ions along with a relatively high water flux at low operating pressure. Most NF membranes are porous and have a negatively charged surface.[7] Separation using charged membranes, either without porosity (swollen gel) or with porosity (fixed charged groups on the pore wall), is based on charge exclusion (the Donnan effect; ions or molecules having the same charge as the fixed ions in the membrane will be rejected, whereas species with opposite charge will be taken up by and transported through the membrane). Therefore, the type of charge and the charge density are the most important characteristics of these membranes. Charged surface porous membranes are more effective in filtration, because of the Donnan effect.[8]

The development of high-performance membranes requires polymers with outstanding properties (i.e., high glass-transition temperature ($T_g$), good mechanical and thermal properties,

excellent chemical stability). Polysulfone (PSf),[9] polyethersulfone (PES),[10] polyaniline (PAN),[11] and cellulose-based polymers[12] are widely used in membrane preparation. Carboxylated polysulfones and sulfonated polysulfones are more effective than PSf,[13] because carboxylation and sulfonation of the polymer leads to hydrophilic and cation exchange membranes.[14] Enhancement of the hydrophilicity in polymeric membrane materials results in membranes with higher flux and better membrane characteristics. Introducing the acid groups in the membrane will increase the enhancement in hydrophilicity.

Polystyrene-alt-maleic anhydride, poly(isobutylene-alt-maleic anhydride) and its derivatives have showed increased interest in recent years, because of their potential applications as drug carrier,[15] nanotechnology,[16,17] biomaterial carrier,[18] and antirejection for cross-species transplantation.[19] Poly(isobutylene-alt-maleic anhydride) (PIAM) has an aliphatic chain and a repeating anhydride group in it, which breaks into two carboxylic acid groups when it comes in contact with water.[20] Carboxylic acid group imparts surface charge to create the Donnan effect. An excess of hydrophilicity of the membrane reduces the mechanical strength and thermal stability but carboxylic groups enhances the hydrophilicity. Consequently, PIAM is considered as an ideal material for nanofiltration membranes. Keeping in view of these points, we hereby report on the convenient preparation of new NF composite membranes of PIAM and polysulfone in different compositions and their characterization by Fourier transform infrared spectroscopy (FT-IR), differential scanning calorimetry

(DSC), contact angle measurement, ion-exchange capacity, water uptake, and also filtration performance study of membranes such as flux and salt rejection.

## ■ EXPERIMENTAL SECTION

**Preparation of Membrane.** Udel polysulfone ($M_w$ = 35 000), poly(isobutylene-alt-maleic anhydride) (PIAM) ($M_w$ = 3000 Da) were obtained from Sigma—Aldrich (India). N-methyl pyrrolidone (NMP) of analytical-grade purity was obtained from Merck, India and was used without further purification. Both PS and PIAM in required amounts were dried in a vacuum oven for 10 h at 55 °C. A specified amount of NMP was added later and heated 60 °C to dissolve the polymer. The solution was continuously stirred for 20 h to obtain the clear solution and completion of dissolution. Furthermore, stirring was stopped for 30 min and the polymer solution was spread on a glass plate using a Doctor's knife at room temperature. The excess of solvent was removed by heating it in a hot air oven for 1 min at 180 °C. The membrane was separated via the phase inversion technique by dipping the glass plate in ice-cold distilled water. The so-obtained membrane was dipped in distilled water for another 24 h and was washed several times with distilled water. Furthermore, the membrane was immersed in 0.1% NaOH solution for 20 h to break the anhydride group of PIAM and was washed and stored in distilled water.[20] Using the above procedure, membranes with different composition of PS and PIAM were prepared and subjected to further characterization (see Figure 1).

**Characterization.** FT-IR spectra were recorded on a spectrophotometer (JASCO, Model FT/IR 4100). Before recording the spectrum, the membrane was dried in desiccators for 24 h. Scanning electron microscopy (SEM) micrographs of membranes were recorded using a field-emission SEM microscope (JEOL, Model JSM-6380LA). The sample was molded on SEM stubs and dried overnight and the surface was coated with gold, using a sputter coating machine. Cross-sectional images were also recorded using the same sample. DSC was used to measure the $T_g$ values. DSC thermograms of dedoped membranes were recorded on a Perkin—Elmer instrument (Pyris 1) at a heating rate of 10 °C min$^{-1}$. Scans were carried out from 30 °C to 300 °C under the absence of atmospheric oxygen.

The swelling behavior of the NF membrane was determined by weight change during swelling in distilled water. NF membranes were thoroughly rinsed with distilled water, and then dried in a desiccator for 24 h. These dried NF membranes were later immersed in distilled water for at least 24 h. The swollen membranes were taken out, and excess water on the surface was gently removed by a blotter. The swollen weights of NF membranes then were quickly measured. Later, NF membranes were again dried under vacuum desiccator for 24 h and weighed. The degree of swelling was calculated using the following formula:

$$\% \text{ swelling} = \left(\frac{w_w - w_d}{w_d}\right) \times 100$$

where $w_w$ and $w_d$ are the weight of swollen and dried NF membranes, respectively.[21]

The contact angle between water and the membrane surface was measured using a FTA-200 dynamic contact angle analyzer, according to the sessile droplet method. Briefly, a water droplet
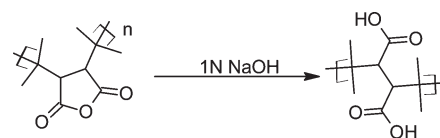


**Figure 1.** Schematic representation of the PIAM polymer after alkali treatment.



1. Nitrogen Cylinder
2. Feed
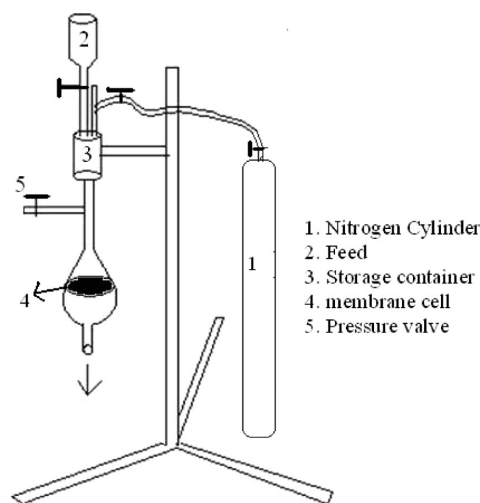3. Storage container
4. membrane cell
5. Pressure valve

**Figure 2.** Schematic diagram of the self-made test cell.

was deposited on a flat homogeneous membrane surface and the contact angle of the droplet with surface was measured. The value was observed until there was no change in contact angle during short measurement period. Each contact angle was measured five times at different points of each membrane sample and an average value was calculated.

The ion exchange capacity (IEC) of the membrane was measured using a conventional titration method. The membrane in H$^+$ form was immersed in a 2 M NaCl solution for 24 h to replace H$^+$ with Na$^+$ completely. The remaining solution was then titrated with 0.01 M of NaOH, using a phenolphthalein indicator. The IEC value was calculated using the following equation:

$$\text{IEC (mmol/g)} = \frac{0.01 \times 1000 \times V_{\text{NaOH}}}{W_d}$$

where $V_{\text{NaOH}}$ is the volume of NaOH solution consumed for titration (given in liters) and $W_d$ is the weight of the dry membrane sample (expressed in grams). The measurements were carried out with an accuracy of 0.001 mmol/g.[22]

All the permeation experiments were performed at room temperature, using a self-constructed dead end desalination cell (see Figure 2). A circular membrane sample with a diameter of 60 mm was placed in the test cell, with the active surface facing toward the incoming feed. The effective membrane diameter was 50 mm. The flux was measured by direct measurement of the permeate flow, in terms of liter per meter square per hour (L m$^{-2}$ h$^{-1}$). The percent salt rejections was determined by comparing the conductivity of feed and permeate solutions; these samples were analyzed for their salt concentration by conductivity measurement. From the results, the percent
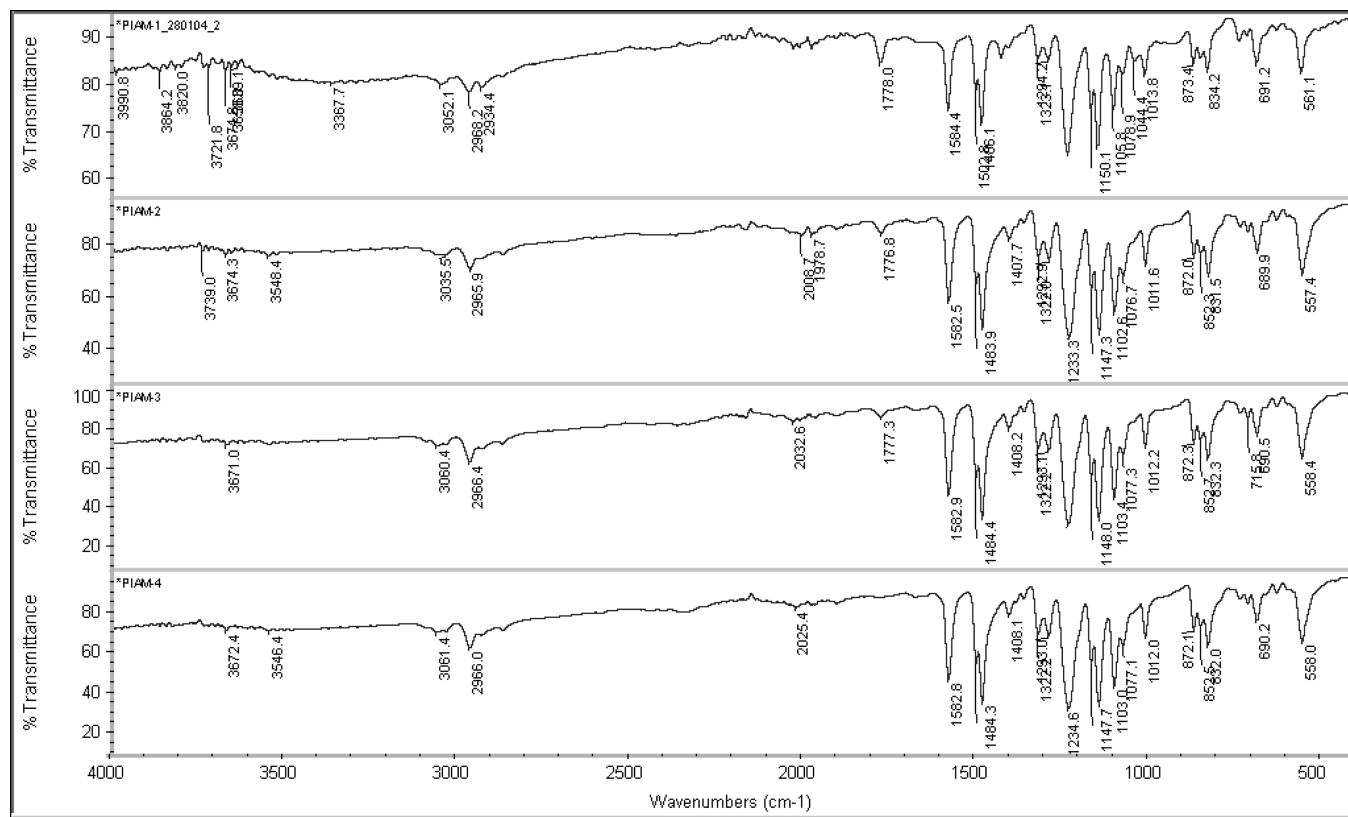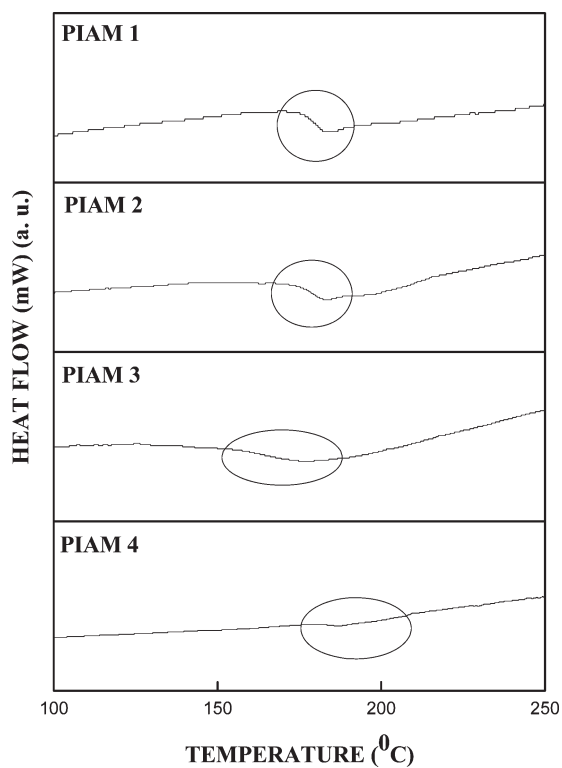
**Figure 3.** Infrared (IR) spectra of membranes.



**Figure 4.** Differential scanning calorimetry (DSC) curve of the membranes.

**Table 1. Membrane Composition with Their Physical Properties**

| sample | membrane composition, PSf:PIAM | membrane code | % water uptake | IEC (mmol/g) | contact angle, $\theta$ |
|---|---|---|---|---|---|
| 1 | 60:40 | PIAM-1 | 54 | 0.98 | 47.40 |
| 2 | 70:30 | PIAM-2 | 50 | 0.97 | 50.68 |
| 3 | 80:20 | PIAM-3 | 20 | 0.69 | 65.97 |
| 4 | 90:10 | PIAM-4 | 14.5 | 0.55 | 67.92 |

retention (% R) was calculated using

$$\% R = \left( 1 - \frac{C_p}{C_f} \right) \times 100$$

where $C_p$ is the salt concentration in the permeate and $C_f$ is the concentration in the feed.[23] Solutions with concentrations of 4000 ppm NaCl, 1000 ppm $Na_2SO_4$, and 1000 ppm $MgSO_4$ were used as feed; the effect of pressure on flux and the percent rejection was studied using the same.

## ■ RESULT AND DISCUSSION

**Characterization of Membrane.** ATR-IR spectra of polymer composites are shown in Figure 3, from which it is clear that as the PIAM concentration increases, the intensity of peak at $\sim$1777 cm$^{-1}$ increases. This can be attributed to an increase in

6530

dx.doi.org/10.1021/ie102387n |Ind. Eng. Chem. Res. 2011, 50, 6528–6534
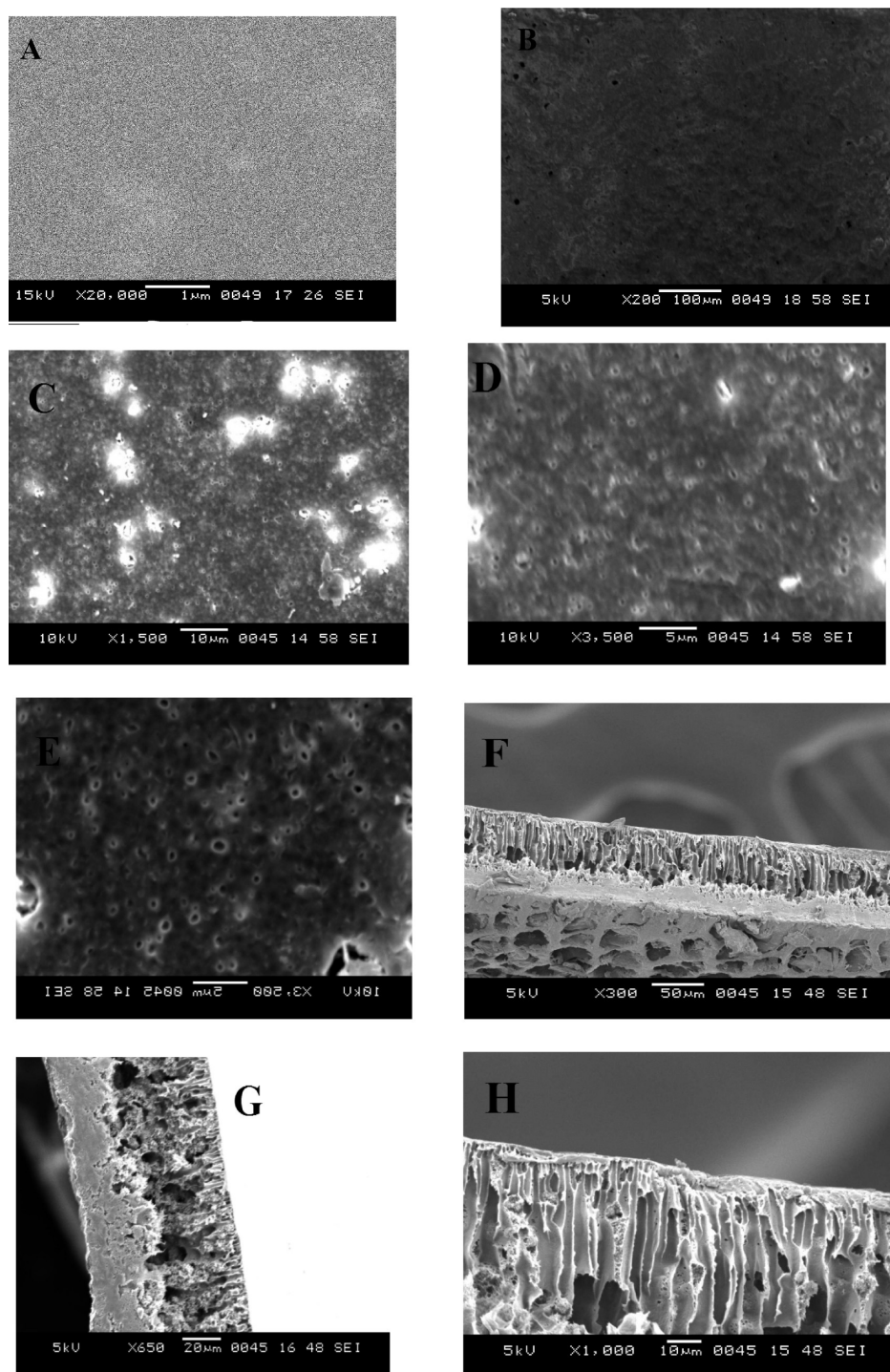
**Figure 5.** SEM images of the membranes showing surface images and cross sections: (A) low-magnification view of the surface image of PIAM-1 after alkali treatment; (B) high-magnification view of the surface image of PIAM-1 after alkali treatment; (C) surface image of PIAM-2; (D) surface image of PIAM-3; (E) surface image of PIAM-4; (F) cross section of PIAM-1; (G) cross section of PIAM-2; and (H) cross section of PIAM-3.

carbonyl group of the composite membrane, and also the peak at $\sim$2966 cm$^{-1}$ can be attributed to $-$OH stretching of the acid group, which also showed an increasing trend as the composition of PIAM increases. This proves that as the composite membrane was dipped in 0.1% NaOH for 20 h, during that NaOH soaking period, the anhydride bond breaks, because of hydrolysis, and forms two acid groups. The presence of a strong peak at $\sim$1235 cm$^{-1}$ is assigned to the ether C$-$O$-$C stretch of the

polysulfone moiety and the peak at $\sim$1147 cm$^{-1}$ is due to O$=$S$=$O stretching.

**Thermal Properties of Membrane.** The thermal behaviors of different blend membranes were studied from the DSC plots. Figure 4 shows the DSC graphs of PIAM membranes. The $T_g$ values of different composite membranes were measured and compared. From the thermal study, it is clear that the $T_g$ value of the blend membrane is different from that of PSf and PIAM alone,

and it also shows a single $T_g$ value. This confirms the formation of a composite, as a result of many van der Waals interactions between two polymers, which lose their identity and show different $T_g$ values that are different from both PIAM and PSf alone. Although the $T_g$ value of PIAM is equal to 141 °C, there is a clear indication that the higher the polysulfone content, the higher the $T_g$ value.

**Swelling Behavior.** Table 1 represents the water uptake results of the membranes as the amount of PIAM increases. This effect was found to be dependent on the presence of long aliphatic chains and carboxylic acid groups in PIAM. Carboxyl groups impart an increase in the hydrogen bonding on the membrane surface. Hence, water uptake will decrease as the PIAM concentration decreases. In PIAM-1, the membrane has 40% PIAM; hence, it shows maximum water uptake.

**Contact-Angle Measurement and Ion-Exchange Capacity.** The contact angle is an important parameter for measuring surface hydrophilicity.[24,25] In general, a smaller contact angle corresponds to more-hydrophilic materials. As can be seen from Table 1, increasing the PIAM concentration decreases the contact angle. However, increasing the PIAM concentration increases the water uptake and IEC. The formation of carboxylic acid groups in the membrane increases as the concentration of PIAM increases. The carboxylic acid group showed enhanced hydrophilicity. PIAM-1 showed a contact angle of 47.40°, and PIAM-4 showed a contact angle of 67.92°. As a result, the membranes are neither hydrophilic nor hydrophobic.

The IEC of the membrane shows the formation of carboxylic acid groups in the membrane. The percentage of PIAM was used less than that of PSf, so the IEC is poor. The measured IEC values are shown in Table 1. PIAM-1 showed a maximum IEC value, whereas PIAM-4 exhibited a smaller IEC value. The IEC decreases as the PIAM concentration decreases.

**Morphology Studies.** SEM is a powerful tool to study the morphology of the membrane. SEM pictures are presented in Figure 5. These micrographs show the morphology of the pure membrane. These morphological features are typically observed in the membrane and are known to be derived from the liquid–liquid phase-demixing process.[26] To develop high-performance polymer membranes, it was essential to design suitable molecule and morphological structures of membranes for their applications. It can be seen from the cross section of these four membranes that they have relatively similar structures, having three layers—a top layer, an intermediate layer, and a sublayer—with finger and spongelike projections; the surface view shows a smooth surface with small pores.

**Performance of the Membrane.** The performances of the membrane experiments were repeated thrice, the difference between all the results were negligible, so mean value of the results have been reported. The results of the membrane before alkaline treatment showed that the rejection of electrolyte solution decreases in the following order: $MgSO_4$, $Na_2SO_4$, and NaCl, as shown in Figures 6 and 7. Higher rejection of $Mg^{2+}$ over $Na^+$ can be explained using the size exclusion principle: $Mg^{2+}$ ions are larger than $Na^+$ ions. Therefore, maximum rejection was exhibited. The rejection results of the membrane after alkaline treatment are presented in Figures 8 and 9. The % rejection of electrolyte solutions decreases in the order of $Na_2SO_4$ > $MgSO_4$ > NaCl, as the performance of the membrane can be explained based on the Donnan effect and the size exclusion mechanism. Donnan exclusion of the electrolyte ions separation occurs at the interaction with fixed charges of the membrane. Because of the formation of carboxylic acid groups on the surface of the membrane
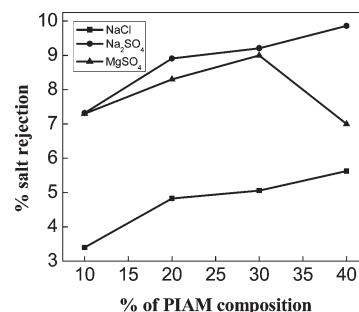


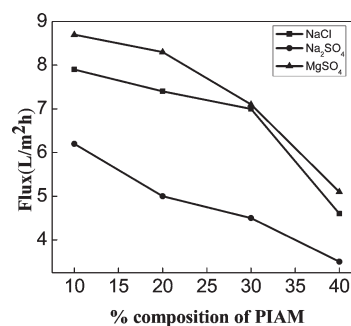**Figure 6.** % Rejection of the membrane before alkali treatment.



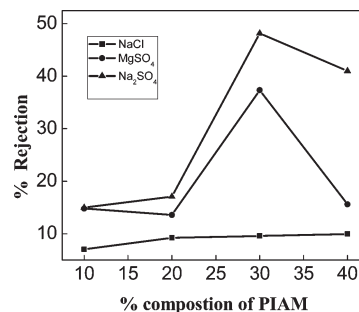**Figure 7.** Flux of the membranes before alkali treatment.



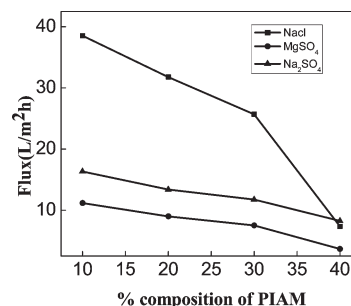**Figure 8.** % Rejection of the membrane after alkali treatment.



**Figure 9.** Flux of the membranes after alkali treatment.

via the breakage of anhydride linkages, cations such as $Na^+$ ions are attracted toward the carboxylate group to create the Donnan effect. Because the size of the $SO_4^{2-}$ ion is larger than that of the $Cl^-$ ion, it cannot pass through the membrane barrier in the case of NaCl, because of the small-sized $Cl^-$ ions, which easily pass through the membrane, because of the Donnan effect to maintain

the charge neutrality across the membrane. However, the $Na^+$ ion will also cross the membrane along with the $Cl^-$ ion. For this reason, $Na_2SO_4$ showed greater rejection than that of NaCl. In addition, the $Na^+$ ion has more affinity toward $COO^-$ than the $Mg^+$ ion, hence, showing greater rejection than $MgSO_4$. Between NaCl and $MgSO_4$, $MgSO_4$ showed greater rejection than NaCl. This is due to the size exclusion mechanism; the $SO_4^{2-}$ ion is larger in size. The concentration of the feed solution is also an important factor in the Donnan effect: if the concentration of the feed sample is more, then the rejection is less. The Donnan effect will increase with an increase in the concentration of PIAM. PIAM-1 contains 40% PIAM polymer, whereas PIAM-4 has 10% PIAM polymer; therefore, the formation of carboxylic acid groups in greater in PIAM-1, so it exhibited greater rejection than the others and rejection decreases with decreasing PIAM polymer concentration. Furthermore, the mobility of the ions across the membranes also plays an important role in the retention rate of ions; the diffusion coefficient and effective size of the ions determine the mobility. According to the diffusion coefficient, $Na_2SO_4$ showed a lower rate than NaCl, because $Na_2SO_4$ shows greater retention.

## ■ CONCLUSION

In the present work, we have prepared new poly(isobutylene-alt-maleic anhydride) (PIAM) and polysulfone composite nanofiltration (NF) membranes of different compositions via the diffusion-induced phase separation (DIPS) method. Membranes were characterized by Fourier transform infrared spectroscopy (FT-IR), scanning electron microscopy (SEM), and differential scanning calorimetry (DSC) studies. These membranes were also tested for salt rejection, flux, and water-swelling studies. These results clearly indicate that, before the alkali treatment, salt rejection and flux was less. However, alkali treatment has resulted in hydrolysis of the anhydride bonds to form the acid groups, which resulted in the formation of nanopores on the membranes. Among the tested salt solutions, $Na_2SO_4$ has showed maximum salt rejection, because of the Donnan effect: the higher the concentration of the PIAM, the higher the salt rejection and the higher the flux due to the increased surface charge (which was due to the carboxylic acid groups formed by base hydrolysis of anhydride bonds). Thermal properties showed that the higher the composition of the polysulfone, the higher the glass-transition temperature ($T_g$) value. The hydrolysis of anhydride bonds via alkaline treatment is a promising method for increasing the flux and the salt rejection of the NF membranes.

## ■ AUTHOR INFORMATION

**Corresponding Author**
*Fax: 91 824 2474033. E-mail: isloor@yahoo.com.

## ■ ACKNOWLEDGMENT

## ■ REFERENCES

(1) Treffry-Goatley, K.; Buckley, C. A.; Groves, G. R. Reverse osmosis treatment and reuse of textile dyehouse effluents. *Desalination* **1983**, *47*, 313–320.

(2) Williams, M. E.; Bhattacharyya, D.; Ray, R. J.; McCray, S. B. Reverse osmosis: Selected applications. In *Membrane Handbook*; Ho, W. S. W., Sirkar, K. K., Eds.; Van Nostrand Reinhold: New York, 1992.

(3) van der Host, H. C.; Timmer, J. M. K.; Robbertsen, T.; Lenders, J. Use of nanofiltration for concentration and demineralization in dairy industry: model for mass transport. *J. Membr. Sci.* **1995**, *104*, 205–218.

(4) Timer, J. M. K.; van der Horst, H. C.; Robbertsen, T. Transport of lactic acid through reverse osmosis and nanofiltration membranes. *J. Membr. Sci.* **1993**, *85*, 205–216.

(5) Timer, J. M. K.; Kromkamp, J.; Robbertsen, T. Lactic acid separation from fermentation broths by reverse osmosis and nanofiltration. *J. Membr. Sci.* **1994**, *92*, 185–197.

(6) Zhou, M. J.; Nemade, P. R.; Lu, X. Y; Zeng, X. H.; Hatakeyama, E. S.; Nobel, R. D.; Gen, D. L. New type of membrane material for water desalination based on cross-linked bicontinuous cubic lyotropic liquid crystal assembly. *J. Am. Chem. Soc.* **2007**, *129*, 9574–9575.

(7) Schaep, J.; Vandecasteele, C. Evaluating the charge of nanofiltration membranes. *Membr. Sci.* **2001**, *188*, 129–136.

(8) Drioli, E.; Giorno, L. *Membrane Operations*; Wiley−VCH Verlag Gmbh & Co. KGaA: Weinheim, Germany, 2009.

(9) Baik, K. J.; Kim, J. Y.; Lee, J. S.; Kim, S. C.; Lee, H. K. Morphology of membranes formed from polysulfone/polyethersulfone/N-methyl-2-pyrrolidone/water system by immersion precipitation. *Korean Polym. J.* **2001**, *9*, 285–291.

(10) Chaturvedi, B. K.; Ghosh, A. K.; Ramachandhran, V.; Trivedi, M. K.; Hanra, M. S.; Misra, B. M. Preparation, characterization and performance of polyethersulfone ultrafiltration membranes. *Desalination* **2001**, *133*, 31–40.

(11) Fan, Z.; Wang, Z.; Daun, M.; Wang, J.; Wang, S. Preparation and characterization of polyaniline/polysulfone nanocomposite ultrafiltration membrane. *J. Membr. Sci.* **2008**, *310*, 402–408.

(12) Kastelan-Kunst, L.; Dananic, V.; Kunst, B.; Kosutic, K. Preparation and porosity of cellulose triacetate reverse osmosis membranes. *J. Membr. Sci.* **1996**, *109*, 223–230.

(13) Chen, M.; Chaio, T.; Tseng, T. Preparation of sulfonated polysulfone/polysulfone and aminated polysulfone/polysulfone blend membranes. *J. Appl. Polym. Sci.* **1996**, *61*, 1205–1209.

(14) Sajitha, C. J.; Mahendran, R; Mohan, D. Studies on cellulose acetate−carboxylated polysulfone blend ultrafiltration membranes— Part I. *Eur. Poly. J.* **2002**, *38*, 2507–2511.

(15) Henry, S. M.; El-Sayed, M. E. H.; Pirie Christopher, M.; Hoffman Allan, S.; Stayton Patrick, S. pH-Responsive poly(styrene-altmaleic anhydride) alkylamide copolymers for intracellular drug delivery. *Biomacromolecules* **2006**, *7*, 2407–2414.

(16) Malardier-Jugroot, C.; van de Ven, T. G. M.; Cosgrove, T.; Richardson, R. M.; Whitehead, M. A. Novel self-assembly of amphiphilic copolymers into nanotubes: Characterization by small angle neutron scattering. *Langmuir* **2005**, *21*, 10179–10187.

(17) Tian, Y.; He, C.; Tao, Y.; Cui, S.; Ai, J.; Li Fabrication of polyethyleneimine and poly(styrene-alt-maleic anhydride) nanotubes through covalent bond. *J. Nanosci. Nanotechnol.* **2006**, *7*, 2072–2076.

(18) Yoshimaga, K.; Kondo, K.; Kondo, A. Capabilities of polymer-modified monodisperse colloidal silica particles as biomaterial carrier. *Colloid Polym. Sci.* **1997**, *275*, 220–226.

(19) Vetere, A.; Donati, I.; Campa, C.; Semeraro, S.; Gamini, A.; Paoletti, S. Synthesis and characterization of a novel glycopolymer with protective activity toward human anti-{alpha}-Gal antibodies. *Glycobiology* **2002**, *4*, 283–290.

(20) Anita, S.; Chan, W.; Micheal, W.; Cecile, M.-J. self-assemble of alternating copolymers and the role of hydrophobic interactions; characterisation by molecular modeling. *Mol. Simul.* **2009**, *1*, 1–9.

(21) Deng, B.; Yang, X.; Xie, L.; Li, J.; Hou, Z.; Yao, S.; Laing, G.; Sheng, K. Microfiltration membranes with pH dependent property prepared from poly(methacrylic acid) grafted polyethersulfone powder. *J. Membr. Sci.* **2009**, *330*, 363–368.

(22) Zhongyi, J.; Xiaohong, Z.; Hong, W.; Fusheng, P. Proton conducting membranes prepared by incorporation of organophosphorus acids into alcohol barrier polymers for direct methanol fuel cells. *J. Power Sources* **2008**, *185*, 85–94.

(23) Lei, L.; Suobo, Z.; Xiaosa, Z. Preparation and characterization of poly(piperazineamide) composite nanofiltration membrane by interfacial polymerization of 3,3′,5,5′-biphenyl tetraacyl chloride and piperazine. *J. Membr. Sci.* **2009**, *335*, 133–139.

(24) Khayet, M.; Feng, C. Y.; Khulbe, K. C.; Matsuura, T. Preparation and characterization of polyvinylidene fluoride hollow fiber membranes for ultrafiltration. *Polymer* **2002**, *43*, 3879–3890.

(25) Palacio, L.; Calvo, J. I.; Prádanos, P.; Hernández, A.; Väisänen, P.; Nyström, M. Contact angles and external protein adsorption onto UF membranes. *J. Membr. Sci.* **1999**, *152*, 189–201.

(26) Lin, D.-J.; Chang, C.-L.; Huang, F.-M.; Chang., L.-P. Effect of salt additives on the formation of microporus Poly(vinylidene floride) membranes by phase inversion from LiClO$_4$/water/DMF/PVDF system. *Polymer* **2003**, *44*, 413–422.

6534

dx.doi.org/10.1021/ie102387n |*Ind. Eng. Chem. Res.* 2011, 50, 6528–6534